

Interpretable Safety Validation for Autonomous Vehicles

Anthony Corso¹, and Mykel J. Kochenderfer¹

Abstract—An open problem for autonomous driving is how to validate the safety of an autonomous vehicle in simulation. Automated testing procedures can find failures of an autonomous system but these failures may be difficult to interpret due to their high dimensionality and may be so unlikely as to not be important. This work describes an approach for finding interpretable failures of an autonomous system. The failures are described by signal temporal logic expressions that can be understood by a human, and are optimized to produce failures that have high likelihood. Our methodology is demonstrated for the safety validation of an autonomous vehicle in the context of an unprotected left turn and a crosswalk with a pedestrian. Compared to a baseline importance sampling approach, our methodology finds more failures with higher likelihood while retaining interpretability.

I. INTRODUCTION

An open problem for autonomous driving is how to validate the safety of an autonomous vehicle (AV) before deploying it on the road. A common practice is to test the AV using a realistic driving simulator that can dynamically control the driving environment. Testing procedures are either white-box, where the tester uses domain knowledge about the AV to generate challenging driving scenarios, or black-box, where no knowledge of the AV or simulator is used. Typically, white-box testing does not scale up due to the manual nature of test case generation, so much of the focus has been on black box testing. Black-box testing is more scalable but the discovered failures are often not interpretable due to the high-dimensionality of the failure examples. In this work we try to address this problem by developing a technique for interpretable black-box testing.

The safety validation problem we study involves finding failures of an autonomous system (system-under-test or SUT) that operates in a stochastic environment. The state of the SUT and the environment is $s \in \mathcal{S}$ and the actions $a \in \mathcal{A}$ are stochastic changes in the environment that can influence the SUT. For autonomous driving, the state is the pose of each agent and the internal state of the AV policy, while the actions may include the behavior of other drivers, the behavior of pedestrians, and sensor noise. An action trajectory $\tau = \{a_1, \dots, a_N\}$ has a probability $p(\tau)$ which models the stochastic elements of the environment. Let the set of all trajectories that end in a failure of the AV be denoted E . The notation $\tau \in E$ means that the sequence of actions τ causes the SUT to fail.

Black-box falsification techniques try to find any τ such that $\tau \in E$. Falsification can be cast as an optimization problem over the space τ [1] which can be solved using

various optimization algorithms [2]–[6]. These approaches do not scale well when τ is long and each action a is high-dimensional. Additionally, if they do find a failure, it might be extremely rare according to $p(\tau)$. Adaptive stress testing [7]–[10] tries to find the most likely failure by maximizing $p(\tau)$ subject to $\tau \in E$ and frames the falsification problem as a Markov decision process so it can be solved using reinforcement learning. Failures can also be found using importance sampling [11]–[13], or with rapidly exploring random trees [14].

For an algorithm to be interpretable, its results must be readily understood by a human. Interpretable models must therefore choose an output representation that is sufficiently expressive to compactly convey the desired information while having direct mappings to words and concepts. Decision trees use a branching set of rules to classify data [15] or represent a reinforcement learning policy [16]. Simple mathematical expressions can be used for regression [17], governing equation discovery [18] and as a reinforcement learning policy [19]. Signal temporal logic (STL) is a representation that is well-suited for high-dimensional time series data because it describes logical relationships between temporal variables and has a natural-language description that is easily understood. STL expressions have been used for the interpretable clustering of multivariate time series data [20], [21].

Our approach seeks to find an interpretable representation (using STL) of an action trajectory τ that causes the SUT to fail. We start with a model of the stochastic elements of the environment $p(\tau)$ and a candidate STL expression that describes an interpretable relationship between these elements. Action trajectories are sampled from $p(\tau)$ such that they satisfy the STL expression and then are simulated. A loss is computed based on the probability of the trajectory and whether it resulted in failure. The STL expression is then optimized according to the loss until we arrive at an expression that reliably causes high-likelihood failures of the SUT. This expression can then be used to generate failure examples (as in black-box testing), as well as understand what features of the environment were important for causing the failure (as in white-box testing).

We use our approach to find the most-likely failures of an autonomous vehicle in two driving scenarios: 1) An unprotected left turn scenario with a small discrete action space, and 2) a crosswalk scenario with a continuous and high-dimensional action space to show that the approach scales. The first scenario uses a simple model for the stochastic actions where each action is independent from the others, while the second scenario uses a Gaussian process

A. Corso and M. J. Kochenderfer are with the Aeronautics and Astronautics Department, Stanford University. e-mail: {acorso,mykel}@stanford.edu

model—a more versatile joint distribution over actions. In both scenarios, we find interpretable failure modes of the AV for several different initial conditions. Additionally, our approach finds an order of magnitude more failures than the importance sampling baseline and the failures that are found have a much higher likelihood.

The main contributions of this paper are:

- 1) An approach for interpretable generative modeling of time series data.
- 2) Application of the approach to finding the most likely failures of an autonomous system.
- 3) Demonstration that our approach outperforms baseline methods for finding failures of an autonomous vehicle in two driving scenarios.

The paper is organized as follows. Section II describes the necessary technical background for our approach. Section III give details of the algorithm. Section IV describes two experiments with safety validation of autonomous vehicles and section V concludes and gives future direction.

II. BACKGROUND

This section provides an overview of topics needed for the remainder the the paper. We discuss signal temporal logic, context-free grammars, genetic programming for expression optimization, and Gaussian processes.

A. Signal Temporal Logic

Signal temporal logic (STL) is a logical formalism that is used to describe the behavior of time-varying systems [22], [23]. STL uses the basic logical propositions *and* (\wedge), *or* (\vee), and *not* (\neg), as well as temporal propositions such as *eventually* (\Diamond) and *always* (\Box). The latter two are defined for sequences of propositions as shown in fig. 1.

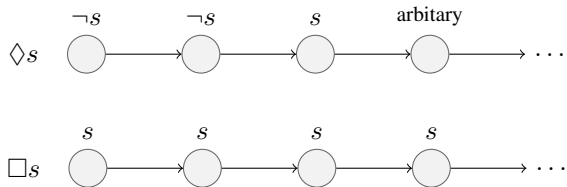


Fig. 1: Definition of eventually and always.

Temporal logic operators are evaluated on series of Booleans. Continuous and discrete time series data are converted to Boolean statements using the comparison operators \leq , \geq , and $=$. A time series τ satisfies an STL expression ψ if $\psi(\tau)$ evaluates to TRUE.

STL statements can also include an explicit dependence on time. The proposition $\Box_{[t_1, t_2]}(x < 10)$ means *always* $x < 10$ for $t \in [t_1, t_2]$ and $\Diamond_{[t_1, t_2]}(x = 13)$ means *eventually* $x = 13$ for $t \in [t_1, t_2]$. The flexibility of STL and the ease with which STL statements can be converted into natural language can make it a suitable choice for interpretable modeling of time heterogeneous time series [20], [21].

B. Context-Free Grammar

A context-free grammar is a set of rules that define a formal language such as STL. Each rule in the grammar is composed of an output type and a set of inputs consisting of types and symbols. To generate an expression, a starting type is chosen and types are recursively expanded until only symbols remain.

The grammar for the STL language described in section II-A is given in eq. (1) for a single time series variable x . The type \mathbb{B} is used for Boolean scalars, \mathbb{S} is for Boolean series, \mathbb{T} is for time, and \mathbb{X} is for values of x . The logical operators apply element-wise on series. The symbol $|$ separates rules on the same line and $:$ indicates a range of symbols. Note that in this work, time is discrete and the variable x may be discrete or continuous. When x is continuous, \mathbb{X} is sampled uniformly at random in the range $[x_{\min}, x_{\max}]$.

$$\begin{aligned}
 \mathbb{B} &\mapsto \mathbb{B} \wedge \mathbb{B} \mid \mathbb{B} \vee \mathbb{B} \mid \neg \mathbb{B} \\
 \mathbb{B} &\mapsto \Box_{[\mathbb{T}, \mathbb{T}]}(\mathbb{S}) \mid \Diamond_{[\mathbb{T}, \mathbb{T}]}(\mathbb{S}) \\
 \mathbb{T} &\mapsto 0 : T_{\max} \\
 \mathbb{S} &\mapsto \mathbb{S} \wedge \mathbb{S} \mid \mathbb{S} \vee \mathbb{S} \mid \neg \mathbb{S} \\
 \mathbb{S} &\mapsto x \leq \mathbb{X} \mid x \geq \mathbb{X} \mid x = \mathbb{X} \\
 \mathbb{X} &\mapsto [x_{\min}, x_{\max}]
 \end{aligned} \tag{1}$$

C. Genetic Programming

Genetic programming is a population-based optimization technique for trees such as expressions generated from a grammar [24], [25]. Trees are evaluated according to a fitness function to determine the quality of an individual. To start the optimization, a population of N_{pop} trees is randomly sampled. Then, the following operations are performed randomly at each iteration (or generation) until convergence:

- **Reproduction:** The fittest tree is selected from a subset of the population and progresses to the next iteration.
- **Mutation:** A random node in the tree is replaced with a random tree of the same type. This operation is applied to a random individual that then progresses to the next iteration.
- **Crossover:** Two individuals are selected at random and mixed to create a child. A random subtree from the first individual replaces a random node of the same type in the second individual. The resulting tree progresses to the next iteration.

D. Gaussian Processes

A Gaussian process [26] is a stochastic process where any finite set of sample points $\mathbf{t} = [t_1, \dots, t_m]$ have values $\mathbf{x} = [x_1, \dots, x_m]$ that are distributed according to a multivariate normal distribution of the form

$$\mathbf{x} \sim \mathcal{N}(\mu(\mathbf{t}), \mathbf{K}(\mathbf{t}, \mathbf{t})) \tag{2}$$

where $\mu_i(\mathbf{t}) = \mu(t_i)$ for mean function μ and $K_{ij}(\mathbf{t}, \mathbf{t}') = k(t_i, t'_j)$ for kernel function k . A common choice for k is the squared exponential kernel with variance σ^2 and characteristic length ℓ given by

$$k_{l, \sigma}(t_1, t_2) = \sigma^2 \exp\left(-\frac{(t_1 - t_2)^2}{2\ell^2}\right). \tag{3}$$

One strength of Gaussian processes is the ability to easily compute a posterior distribution after observing some values \mathbf{x}^o at observation points \mathbf{t}^o .

To apply linear constraints on a Gaussian process, we use the procedure of Jidling *et al.* [27] where they apply a transformation to sample points from a truncated multivariate normal distribution. Sampling from a truncated multivariate distribution can be done efficiently with the minimax tilting approach [28]. For notational convenience, we write a Gaussian process with mean μ , kernel k , observed points \mathbf{x}^o , lower bound linear constraints \mathbf{l} and upper bound linear constraints \mathbf{u} as

$$\mathcal{GP}(\mu, k, \mathbf{x}^o, \mathbf{l}, \mathbf{u}). \quad (4)$$

III. METHODS

This section introduces a method for interpretable generative modeling of time series based on STL. First, we give an overview of the algorithmic approach to optimizing STL expressions. Next, we discuss how expressions are generated and how time series are sampled from them.

A. Algorithm Overview

The procedure for optimizing STL expressions is represented by the flow diagram in fig. 2. STL expressions are sampled from an STL grammar. Many expressions may be sampled simultaneously if a population-based optimization procedure is used. The STL expressions are then converted into constraints on the time series data. The constraints are generated so that any time series that satisfies them will also satisfy the corresponding STL expression. Note that there are many different constraints that could enforce a time series to satisfy an STL expression, some more restrictive than others. As explained in section III-C, we will sample from the set of constraints that impose the minimal amount of restriction on the time series but still enforce satisfaction. Next, a probability model over the time series is used in conjunction with the constraints to generate random time series samples that satisfy each STL expression. A problem-dependent loss for the STL expression is computed from the time series samples and the optimizer uses it to improve the STL expressions that are sampled on the next iteration. The process repeats until a maximum number of iterations is reached or an STL expression is found that has a sufficiently low loss.

B. Sampling Expressions

Expressions need to be sampled from the STL grammar during the initialization of the genetic programming optimization scheme and during the mutation procedure. Feasible rules from the STL grammar are selected uniformly at random during each node expansion. A maximum depth of 10 is imposed on all expressions to keep them from becoming too large. The grammar is defined and sampled from using ExprRules.jl.

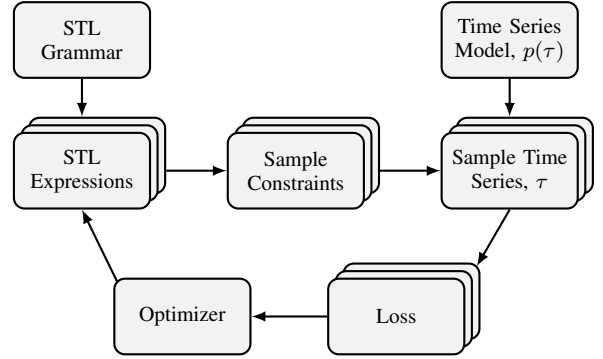


Fig. 2: Overview of the optimization loop for our approach.

C. Converting Expressions into Stochastic Constraints

For an STL expression to be used as a generative model, we need to be able to efficiently sample time series that satisfy the expression. A naive approach would be to sample time series according to the probability model and then reject the samples that do not satisfy the expression. If the expression places very restrictive requirements on the feasible time series, then a prohibitive number of samples would be required to find one that satisfies the expression.

To mitigate this problem, we construct linear constraints for each STL expression that are imposed on sampled time series, enforcing the satisfaction of the STL expression. There are efficient algorithms for sampling from certain linearly-constrained distributions [27], which makes this approach tractable.

There are many different constraints that could enforce a time series to satisfy an STL expression. We seek to find the set of constraints that impose the minimum restriction on the time series (while enforcing STL satisfaction), and choose one of these constraints at random. The procedure for sampling the minimally-restrictive constraints is given in algorithm 1. The algorithm relies on sampling from the set of feasible inputs for each temporal logic proposition. The inputs to each proposition can be TRUE, FALSE, or ARBITRARY, where ARBITRARY means that there is no restriction placed on what the input can be. When sampling feasible inputs, we want to place the minimum amount of restrictions so ARBITRARY is used whenever possible. The minimally-constrained feasible inputs for each STL proposition are given in table I

The algorithm proceeds in a top-down fashion starting with the highest level expression. Sequences of Booleans are found that satisfy that expression. For example, if the expression $\square_{[1,3]}(s)$ evaluates to FALSE, then, according to table I, a random point in $t_i \in [1, 3]$ would be chosen such that $s(t_i) = \text{FALSE}$. The other Booleans in the sequence would be ARBITRARY. If s is composed of STL expressions, they are handled in the same way, using the output of s as their evaluation target. Once an output is ARBITRARY, then all inputs that are descendants of that expression will be ARBITRARY as well. Ultimately, the STL expressions terminate in comparison operations that make up the constraints.

If the statement $x \leq 5$ evaluates to TRUE at t_1 , then we would impose the linear constraint that $x^{(1)} \leq 5$. If the same statement evaluates to ARBITRARY, then no constraint would be imposed.

To illustrate the construction of stochastic constraints more clearly, consider the following complete example. Suppose we wish to sample a 3-step time series that satisfies the STL expression

$$\diamondsuit_{[1,3]}((x \leq 3) \wedge (y = 0)). \quad (5)$$

We begin by selecting from the possible inputs to the top level expression $\diamondsuit_{[1,3]}$. Consulting table I, we find the following possibilities

$$[T, A, A] \quad [F, T, A] \quad [F, F, T]. \quad (6)$$

After choosing randomly, suppose we select $[F, T, A]$, which corresponds to S in algorithm 1. Each Boolean in the series is the result of the expression $(x \leq 3) \wedge (y = 0)$, which corresponds to I in algorithm 1. Consulting table I again, we find that the first entry could result from inputs (F, A) or (A, F) . The second entry had to come from (T, T) , and the remaining entry has arbitrary inputs. Choosing at random, we could end up with the following inputs to the \wedge operation

$$([F, T, A], [A, T, A]) \quad (7)$$

The first input corresponds to the statement $x \leq 3$ and the second input corresponds to the statement $y = 0$. We therefore arrive at the following constraints for each step of the time series

$$[x > 3, x < 3 \wedge y = 0, \text{none}, \text{none}]. \quad (8)$$

These constraints are then imposed on the probability model during sampling to ensure that the time series satisfies the STL expression.

Algorithm 1 Sample constraints from an expression ex for known output out , and store the results in an array C

```

procedure SAMPLECONSTRAINTS( $ex, out, C$ )
  if  $ex$  is a constraint
    push( $C, (ex, out)$ )
  else ▷ Then  $ex$  is a proposition
     $S \leftarrow \text{SampleFeasibleInputs}(ex, out)$ 
     $I \leftarrow \text{InputExpressions}(ex)$ 
    for  $i$  in  $1:\text{length}(I)$ 
      SampleConstraints( $I[i], S[i], C$ )
  
```

D. Sampling Multivariate Time Series with Constraints

Let $[\mathbf{x}^{(1)}, \dots, \mathbf{x}^{(m)}]$ be a multivariate times series with m samples of $\mathbf{x} \in \mathbb{R}^n$. Suppose we are given a set of constraint functions $\mathbf{l}, \mathbf{u} : \mathbb{R} \rightarrow \mathbb{R}^n$ such that $\mathbf{l}_j(t) \leq x_j(t) \leq \mathbf{u}_j(t)$ and $\mathbf{l}_j(t) \leq u_j(t)$ for $j = 1, \dots, n$. The most general model of this times series is given by the joint probability distribution

$$p(\mathbf{x}^{(1)}, \dots, \mathbf{x}^{(m)}) \quad (9)$$

TABLE I: The minimally restrictive feasible inputs for the desired output of an expression. T, F, and A are TRUE, FALSE, and ARBITRARY.

Proposition	Output	Feasible Input
\wedge	TRUE	(T, T)
	FALSE	(F, A) or (A, F)
\vee	TRUE	(T, A) or (A, T)
	FALSE	(F, F)
\neg	TRUE	F
	FALSE	T
$\square_{[t_1, t_2]}$	TRUE	[A, ..., $\underbrace{T, \dots, T}_{[t_1, t_2]}, A, \dots]$
	FALSE	[A, ..., $\underbrace{F, \dots, F}_{t \in [t_1, t_2]}, A, \dots]$
$\diamondsuit_{[t_1, t_2]}$	TRUE	[A, ..., $\underbrace{F, \dots, T}_{t_1, t \in [t_1, t_2]}, A, \dots]$
	FALSE	[A, ..., $\underbrace{F, \dots, F}_{[t_1, t_2]}, A, \dots]$

with the imposed constraint

$$\mathbf{l}(t_i) \leq \mathbf{x}^{(i)} \leq \mathbf{u}(t_i) \quad (10)$$

where t_i corresponds to the time of the sample point $\mathbf{x}^{(i)}$. The model p captures the correlations in the data over time and between variables.

If time series samples are independent, then the probability distribution decomposes to

$$p(\mathbf{x}^{(1)}, \dots, \mathbf{x}^{(m)}) = \prod_{i=1}^m p(\mathbf{x}^{(i)}) \quad (11)$$

When the components of \mathbf{x} are also independent, it decomposes further to

$$\prod_{i=1}^m p(\mathbf{x}^{(i)}) = \prod_{i=1}^m \prod_{j=1}^n p(x_j^{(i)}) \quad (12)$$

If the probability model is uniform, the j th component of the sample at t_i is distributed as

$$x_j^{(i)} \sim \mathcal{U}(l_j(t_i), u_j(t_i)) \quad (13)$$

If the probability model of the j th component is normal with mean $\tilde{\mu}_j$ and variance $\tilde{\sigma}_j^2$, then the sample at t_i is distributed as a truncated normal distribution

$$x_j^{(i)} \sim \mathcal{TN}_{l_j(t_i), u_j(t_i)}(\tilde{\mu}_j, \tilde{\sigma}_j^2) \quad (14)$$

When the time series is jointly distributed as a Gaussian process with mean function μ_j and kernel k_j for the j th component, then samples are distributed according to

$$[x_j^{(1)}, \dots, x_j^{(m)}] \sim \mathcal{GP}(\mu_j, k_j, l_j(\mathbf{t}^o), l_j(\mathbf{t}^c), u_j(\mathbf{t}^c)) \quad (15)$$

The inequality constraints are separated into two sets: \mathbf{t}^o where $l_j(\mathbf{t}^o) = u_j(\mathbf{t}^o)$ and \mathbf{t}^c where $l_j(\mathbf{t}^c) < u_j(\mathbf{t}^c)$.

IV. EXPERIMENTS

This section describes experiments that use our approach to find failures of an autonomous vehicle in two driving scenarios: 1) an unprotected left turn, and 2) a vehicle approaching a crosswalk with a pedestrian. The driving scenarios were designed with `AutomotiveDrivingModels.jl`, an open-source Julia package. The system-under-test is an AV (referred to as the ego vehicle) that follows a modified version of the intelligent driver model (IDM) [29]. The IDM is a vehicle-following algorithm that tries to drive at a specified velocity while avoiding collisions with leading vehicles or pedestrians. In our experiments, the IDM is parameterized by a desired velocity of 29 m/s, a minimum spacing of 5 m, a maximum acceleration of 3 m/s² and a comfortable braking deceleration of 2 m/s². In the left-turn scenario, the IDM is augmented with a rules-based algorithm for navigating the intersection that predicts the behavior of oncoming traffic based on turn signals and right-of-way norms.

In both driving scenarios, we aim to find the most likely failures of the SUT based on the models of the environment, where a failure is any collision between the ego vehicle and another agent. The performance of our algorithm is evaluated on three metrics: 1) The number of failures generated (per 100 rollouts) from the final STL expressions, 2) the likelihood of the failure trajectories, and 3) the interpretability of the STL expression. As a baseline, we use importance sampling to make finding failures more likely. The importance sampling distribution for each scenario will be described below.

The number of failures was computed by sampling 100 trajectories (either from the optimal STL expression or the IS distribution) and counting the number of failures. The trajectory probability was computed by finding 100 failure trajectories for each method and averaging their likelihood. The number of failures and trajectory probability were computed from 5 trials so the sample mean and standard deviation are reported.

In all of the experiments, the STL optimization was performed with genetic programming with a population of 1000 individuals over 30 generations, implemented in `ExprOptimization.jl`. The probability of reproduction was 0.3, the probability of crossover was 0.3 and the probability of mutation was 0.4. The loss function for a sequence of actions τ was $\mathcal{L}(\tau) = -p(\tau)\mathbb{1}\{\tau \in E\}$. When minimized, this loss produces the highest likelihood failure trajectory.

A. Two-vehicle Interaction

As shown in figs. 3 to 5, the first scenario is an interaction between the ego vehicle, which is attempting to turn left, and one adversarial vehicle which is initially driving straight through the intersection. The yellow dot represents a turn signal. The adversarial vehicle has a discretized action space with seven possible actions shown in table II. The actions act as disturbances to the normal behavior of the vehicle dictated by the IDM. The adversarial vehicle may do nothing, change its acceleration, toggle its turn signal, or change whether or

TABLE II: Action space and probability models for adversarial vehicle

Action	Symbol	Acceleration	Probability
No Disturbance	0	0 m/s ²	0.976
Medium deceleration	d_{med}	-1.5 m/s ²	1×10^{-2}
Major deceleration	d_{maj}	-3 m/s ²	1×10^{-3}
Medium acceleration	a_{med}	1.5 m/s ²	1×10^{-2}
Major acceleration	a_{maj}	3 m/s ²	1×10^{-3}
Toggle blinker	B	N/A	1×10^{-3}
Toggle turn intent	L	N/A	1×10^{-3}

not it will turn or go straight. As shown in table II, each action has an associated probability with larger disturbances being less likely. Under this probability model, failures are very unlikely to occur so we use importance sampling (IS) as a baseline. The accelerating distribution was chosen to be uniform over the actions. The simulation timestep was set to $\Delta t = 0.18$ s.

Three initial conditions of the left-turn (LT) scenario were investigated. The initial conditions and corresponding nominal behavior of the ego vehicle are given below.

- LT #1: Ego vehicle is 15 m below the intersection, going 9 m/s. The adversarial vehicle is 29 m left of the intersection and is going 10 m/s. The nominal behavior is for the ego vehicle to take the left turn before the other vehicle arrives at the intersection.
- LT #2: Ego vehicle is 15 m below the intersection, going 9 m/s. The adversarial vehicle is 29 m left of the intersection and is going 20 m/s. The nominal behavior is for the ego vehicle to wait for other vehicle to pass through the intersection before turning left.
- LT #3: Ego vehicle is 19 m below the intersection, going 9 m/s. The other vehicle is 43 m left of the intersection and is going 29 m/s. The nominal behavior is the same as in LT #2.

The results for the three initial conditions are shown in table III. Action sequences that were sampled from the optimal STL expression produced at least an order of magnitude more failures than the rollouts from the IS distribution. This means that once the optimal expression is computed, it is very effective at generating failures. Additionally, we see that the average action probability is much higher for the interpretable failures than for the IS failures. The interpretable failures place minimal constraints on the trajectories so many of the actions are selected according to the true model of the environment, leading to the relatively high likelihood of the trajectory. With importance sampling, the distribution we use causes rare actions to be chosen with regularity, even when they are not critical for causing a failure. Many rare events cause the IS trajectories to have very low likelihood.

Finally, we can interpret the failure STL expressions generated by the genetic algorithm. For LT #1, we see that the optimal STL expression enforces a major acceleration in the first two timesteps of the simulation. This acceleration allows the adversarial vehicle to just reach the ego vehicle as it completes its left turn as shown in fig. 3 (ego vehicle

TABLE III: Comparing STL (our approach) to importance sampling (IS) for three different initial conditions of the left-turn scenario.

	Method	No. of Failures	Traj. Prob.	Expression
LT #1	STL	96.80 \pm 2.77	0.78 \pm 0.049	$\square_{[0,..36]} a_{\text{maj}}$
	IS	0.80 \pm 0.84	0.11 \pm 0.099	-
LT #2	STL	99.40 \pm 1.34	0.82 \pm 0.049	$\square_{[0,0]} B$
	IS	9.20 \pm 3.63	0.15 \pm 0.13	-
LT #3	STL	16.40 \pm 4.28	0.75 \pm 0.029	$\square_{[0,..36]} B \vee d_{\text{maj}}$
	IS	1.80 \pm 0.45	0.15 \pm 0.13	-

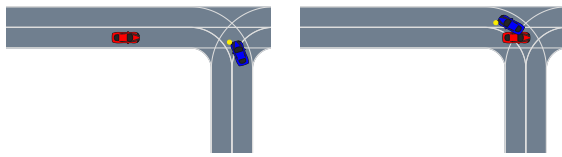


Fig. 3: Collision for LT #1 at $t = (1.08\text{s}, 1.98\text{s})$.

in blue). The ego vehicle initiated the turn based on the initial velocity of the other vehicle and did not predict such a significant speedup. For LT # 2, the optimal STL expression simply has the adversarial vehicle turn on its blinker but to still travel straight through the intersection as shown in fig. 4. The ego vehicle expects the adversarial vehicle to turn, so it initiates the left turn and causes a collision. Lastly, for LT #3, the optimal STL expression has the vehicle either turn on its turn signal or perform a major deceleration in the first two timesteps of the simulation. This leads to a collision only 16.40 out of 100 trials but demonstrates that this failure mode requires both a deceleration and an incorrect turn signal as shown in fig. 5. From these experiments, we conclude that our approach is able to find interpretable STL expressions that reliably produce likely failures of the SUT.

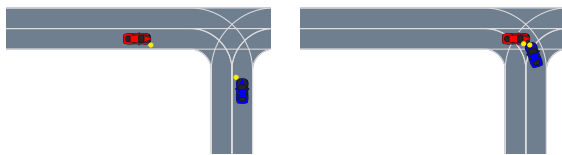


Fig. 4: Collision for LT #2 at $t = (0.72\text{s}, 1.26\text{s})$.

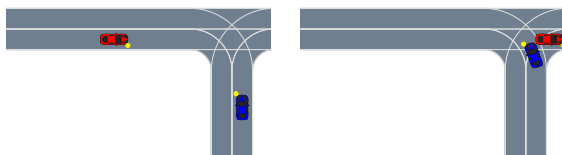


Fig. 5: Collision for LT #3 at $t = (0.90\text{s}, 1.62\text{s})$.

B. Pedestrian Crosswalk Interaction

As shown in figs. 6 and 7, the second driving scenario has an autonomous vehicle approach a crosswalk while a pedestrian tries to cross, as done by Koren *et al.* [8]. The stochastic actions we control are the the pedestrian acceleration (a_x, a_y), the sensor noise on pedestrian position (n_x, n_y), and the sensor noise on the pedestrian velocity (n_{v_x}, n_{v_y}). The sensor noise is modeled as independent samples from a zero-mean Gaussian with standard deviations σ_{pos} for the position noise in both directions and σ_{vel} for the velocity noise in both directions. The pedestrian acceleration in both directions was modeled as a zero-mean Gaussian process with a squared-exponential kernel. The characteristic length was chosen as $t = 0.4\text{s}$ so that the pedestrian cannot change acceleration too quickly. The standard deviation of the kernel is σ_{acc} . The importance sampling distribution used the same action models but doubled the standard deviation parameters to make larger disturbances more likely. The comparisons in the STL statements were sampled uniformly from $[-2\text{ m/s}^2, 2\text{ m/s}^2]$ for acceleration, $[-1\text{ m}, 1\text{ m}]$ for position noise, and $[-2\text{ m/s}, 2\text{ m/s}]$ for velocity noise.

For these experiments, the vehicle starts 35 m to the left of the crosswalk travelling at 11.7 m/s and the pedestrian starts 4 m below the center of the lane, moving at 1.5 m/s to cross the street. The simulation timestep was set to $\Delta t = 0.2$. The correct behavior for the ego vehicle is to come to a safe stop before the crosswalk as the pedestrian crosses. The difference between pedestrian crosswalk (PC) scenarios is in the choice of probability parameters. The first set of parameters (PC #1) makes pedestrian motion more volatile than sensor noise with $\sigma_{\text{acc}} = 1\text{ m/s}^2$, $\sigma_{\text{pos}} = 0.2\text{ m}$, $\sigma_{\text{vel}} = 0.5\text{ m/s}^2$. The second set (PC #2) causes the noise to be a larger factor with $\sigma_{\text{acc}} = 1\text{ m/s}^2$, $\sigma_{\text{pos}} = 1\text{ m}$, $\sigma_{\text{vel}} = 1\text{ m/s}^2$.

The results of the experiments are shown in table IV and they are similar to the results of the previous experiments. In scenario PC #1 and PC #2, our approach found STL statements that produced failures 100% of the time, an order of magnitude larger than the importance sampling approach. Additionally, the failures found via STL expressions had much higher likelihood than those found using importance sampling. In PC #1 we see that the optimal STL expression prescribes a specific acceleration for the pedestrian that causes the pedestrian to enter the street and hit the car right as the car passes by the crosswalk, as shown in fig. 6. Note that the actual pedestrian position and orientation is shown in red and the vehicle's perceived position and orientation is in gray. In PC #2, the expression also includes some prescribed noise that causes the AV to misjudge the location of the pedestrian as shown in fig. 7. We conclude from these results that our approach performs well with continuous action spaces and complex probability models. It is able to find STL expressions that reliably produce likelier failures than the importance sampling baseline.

V. CONCLUSION

In this work we presented an approach for finding interpretable failures of an autonomous system based on signal

TABLE IV: Comparing STL (our approach) to importance sampling (IS) for two different models of the pedestrian crosswalk scenario

	Method	No. of Failures	Action Prob.	Expression
PC #1	STL	100 ± 0.0	0.0094 ± 0.0	$\square_{[0,3.8]}(a_x = 0.019 \wedge a_y = -0.026)$
	IS	13.4 ± 4.28	$5.24 \times 10^{-32} \pm 5.2 \times 10^{-31}$	N/A
PC #2	STL	100 ± 0.0	$1.26 \times 10^{-23} \pm 7.38 \times 10^{-39}$	$\square_{[0,3.8]}(a_x = -0.32 \wedge a_y = -0.27 \wedge n_{v_y} = 0.26)$
	IS	8.4 ± 1.34	$6.83 \times 10^{-56} \pm 6.78 \times 10^{-55}$	N/A

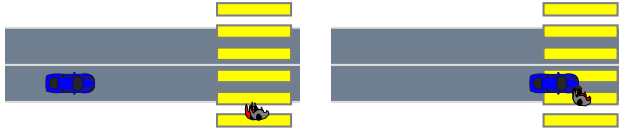


Fig. 6: Collision for PC #2 $t = (1.6 \text{ s}, 3.0 \text{ s})$.

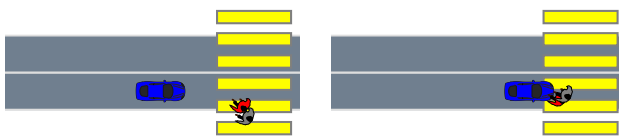


Fig. 7: Collision for PC #2 $t = (2.4 \text{ s}, 3.2 \text{ s})$.

temporal logic. The approach uses genetic programming to optimize an STL expression so that it describes action trajectories that cause an autonomous system to fail. We demonstrated the approach on two autonomous driving scenarios with both discrete and continuous action spaces. We also demonstrated that the technique works in the simplest case of actions that are independent at each timestep, and in the more complex (and more flexible) situation where the actions are jointly distributed as a Gaussian process. Compared to an importance sampling baseline, we found that our approach found an order of magnitude more failures of the autonomous vehicle and those failures had a higher likelihood. We interpreted the found failures to identify flaws in the autonomous vehicle. Future work will include techniques for ensuring good coverage of the input space, and improved optimization techniques. Additionally, we will apply the approach to larger-scale safety validation problems with more complex environments and levels of autonomy.

REFERENCES

- [1] A. Donz and O. Maler, “Robust satisfaction of temporal logic over real-valued signals,” in *International Conference on Formal Modeling and Analysis of Timed Systems (FORMATS)*, 2010.
- [2] L. Mathesen, S. Yaghoubi, G. Pedrielli, and G. Fainekos, “Falsification of cyber-physical systems with robustness uncertainty quantification through stochastic optimization with adaptive restart,” English (US), in *IEEE Conference on Automation Science and Engineering (CASE)*, Aug. 2019.
- [3] T. Akazaki, S. Liu, Y. Yamagata, Y. Duan, and J. Hao, “Falsification of cyber-physical systems using deep reinforcement learning,” in *International Symposium on Formal Methods*, 2018.
- [4] Q. Zhao, B. H. Krogh, and P. Hubbard, “Generating test inputs for embedded control systems,” *IEEE Control Systems Magazine*, vol. 23, no. 4, pp. 49–57, 2003.
- [5] Z. Zhang, G. Ernst, S. Sedwards, P. Arcaini, and I. Hasuo, “Two-layered falsification of hybrid systems guided by monte carlo tree search,” *IEEE Transactions on Computer-Aided Design of Integrated Circuits and Systems (TCAD)*, vol. 37, no. 11, pp. 2894–2905, 2018.
- [6] S. Sankaranarayanan and G. Fainekos, “Falsification of temporal properties of hybrid systems using the cross-entropy method,” in *ACM international conference on Hybrid Systems: Computation and Control (HSCC)*, 2012.
- [7] R. Lee, M. J. Kochenderfer, O. J. Mengshoel, G. P. Brat, and M. P. Owen, “Adaptive stress testing of airborne collision avoidance systems,” in *Digital Avionics Systems Conference (DASC)*, 2015.
- [8] M. Koren, S. Alsaif, R. Lee, and M. J. Kochenderfer, “Adaptive stress testing for autonomous vehicles,” in *IEEE Intelligent Vehicles Symposium (IV)*, 2018.
- [9] A. Corso, P. Du, K. Driggs-Campbell, and M. J. Kochenderfer, “Adaptive stress testing with reward augmentation for autonomous vehicle validation,” in *IEEE International Conference on Intelligent Transportation Systems (ITSC)*, 2019.
- [10] M. Koren and M. Kochenderfer, “Efficient autonomy validation in simulation with adaptive stress testing,” in *IEEE International Conference on Intelligent Transportation Systems (ITSC)*, Oct. 2019.
- [11] Z. Huang, M. Arief, H. Lam, and D. Zhao, “Evaluation uncertainty in data-driven self-driving testing,” in *IEEE International Conference on Intelligent Transportation Systems (ITSC)*, 2019.
- [12] M. O’Kelly, A. Sinha, H. Namkoong, R. Tedrake, and J. C. Duchi, “Scalable end-to-end autonomous vehicle testing via rare-event simulation,” in *Advances in Neural Information Processing Systems (NIPS)*, 2018.
- [13] J. Uesato, A. Kumar, C. Szepesvari, T. Erez, A. Ruderman, K. Anderson, N. Heess, P. Kohli, *et al.*, “Rigorous agent evaluation: An adversarial approach to uncover catastrophic failures,” *ArXiv*, 2018.
- [14] M. Koschi, C. Pek, S. Maierhofer, and M. Althoff, “Computationally efficient safety falsification of adaptive cruise control systems,” in *IEEE International Conference on Intelligent Transportation Systems (ITSC)*, 2019.
- [15] L. Breiman, *Classification and regression trees*. Routledge, 2017.
- [16] I. D. J. Rodriguez, T. Killian, S.-H. Son, and M. Gombolay, “Interpretable reinforcement learning via differentiable decision trees,” *ArXiv*, no. 1903.09338, 2019.
- [17] H. Schielzeth, “Simple means to improve the interpretability of regression coefficients,” *Methods in Ecology and Evolution*, vol. 1, no. 2, pp. 103–113, 2010.
- [18] S. L. Brunton, J. L. Proctor, and J. N. Kutz, “Discovering governing equations from data by sparse identification of nonlinear dynamical systems,” *Proceedings of the National Academy of Sciences*, vol. 113, no. 15, pp. 3932–3937, 2016.
- [19] D. Hein, A. Hentschel, T. Runkler, and S. Udluft, “Particle swarm optimization for generating interpretable fuzzy reinforcement learning policies,” *Engineering Applications of Artificial Intelligence*, vol. 65, pp. 87–98, 2017.
- [20] R. Lee, M. J. Kochenderfer, O. J. Mengshoel, and J. Silbermann, “Interpretable categorization of heterogeneous time series data,” in *SIAM International Conference on Data Mining*, 2018.
- [21] M. Vazquez-Chanlatte, J. V. Deshmukh, X. Jin, and S. A. Seshia, “Logical clustering and learning for time-series data,” in *International Conference on Computer Aided Verification*, 2017.
- [22] O. Maler and D. Nickovic, “Monitoring temporal properties of continuous signals,” in *Formal Techniques, Modelling and Analysis of Timed and Fault-Tolerant Systems*. Springer, 2004, pp. 152–166.
- [23] C. Baier and J.-P. Katoen, *Principles of model checking*. MIT Press, 2008.

- [24] M. J. Kochenderfer and T. A. Wheeler, *Algorithms for optimization*. MIT Press, 2019.
- [25] J. R. Koza, *Genetic programming: On the programming of computers by means of natural selection*. MIT Press, 1992, vol. 1.
- [26] C. E. Rasmussen, “Gaussian processes in machine learning,” in *Summer School on Machine Learning*, 2003.
- [27] C. Jidling, N. Wahlstrm, A. Wills, and T. B. Schn, “Linearly constrained Gaussian processes,” in *Advances in Neural Information Processing Systems (NIPS)*, 2017.
- [28] Z. I. Botev, “The normal law under linear restrictions: Simulation and estimation via minimax tilting,” *Journal of the Royal Statistical Society: Series B*, vol. 79, no. 1, pp. 125–148, 2017.
- [29] M. Treiber, A. Hennecke, and D. Helbing, “Congested Traffic States in Empirical Observations and Microscopic Simulations,” *Physical Review E*, vol. 62, pp. 1805–1824, 2000.